Turing pattern formation with fractional diffusion and fractional reactions

T.A.M. Langlands[1], B.I. Henry[1] and S.L. Wearne[2]

[1] Department of Applied Mathematics, School of Mathematics, University of New South Wales, Sydney NSW 2052, Australia

[2] Center of Biomathematical Sciences, Fishberg Department of Neuroscience, Computational Neurobiology and Imaging Center, Mount Sinai School of Medicine, New York, New York. 10029-6574

Abstract. We have investigated Turing pattern formation through linear stability analysis and numerical simulations in a two-species reaction-diffusion system in which a fractional order temporal derivative operates on both species, and on both the diffusion term and the reaction term. The order of the fractional derivative affects the time onset of patterning in this model system but it does not affect critical parameters for the onset of Turing instabilities and it does not affect the final spatial pattern. These results contrast with earlier studies of Turing pattern formation in fractional reaction-diffusion systems with a fractional order temporal derivative on the diffusion term but not the reaction term.

In addition to elucidating differences between these two model systems our studies provide further evidence that Turing linear instability analysis is an excellent predictor of both the onset of and the nature of pattern formation in fractional nonlinear reaction-diffusion equations.

PACS numbers: 05.40.-a,05.60.Cd,82.40.Ck,82.39.Rt,89.75.Kd

1. Introduction

In recent years, there has been a rapid proliferation in experimental findings of anomalous sub-diffusion reported in materials physics [1, 2], biophysics [3, 4] and econophysics [5]. Anomalous sub-diffusion is characterized by sublinear power law scaling of mean square displacements and heavy tailed probability density functions. The formalism of continuous time random walks (CTRWs) [6, 7], i.e., random walks in which the waiting time between successive steps and the length of the steps are both random variables, has proven a useful starting point for developing theoretical models of systems with anomalous diffusion. One of the most successful paradigms to emerge from this research has been fractional calculus models for anomalous diffusion [8, 9, 10]. In the CTRW model, anomalous sub-diffusion arises when the asymptotic long time limit of the waiting time probability density function is heavy tailed, ie., $\psi(t) \sim t^{-\alpha-1}$ with $0 < \alpha < 1$. The evolution equation for the concentration of non-reacting species undergoing sub-diffusion can then be modelled using a time-fractional diffusion equation which differs from the conventional diffusion equation in that it has a fractional order temporal derivative operating on the spatial Laplacian [8].

A natural generalization is to consider fractional reaction diffusion models for the concentration of species undergoing sub-diffusion and reactions. In the case of standard diffusion with reactions the two effects can be combined additively in a mean field model with the term for reactions represented by a functional form derived from the law of mass action [11, 12]. Standard reaction-diffusion equations have proven useful in many fields including nerve cell signalling [13], animal coat patterns [14], population dispersal [15], and chemistry [16]. One possible generalization of the fractional sub-diffusion equation, to incorporate reactions, is to add a reaction term to the fractional diffusion term [17, 18, 19, 20, 21, 22, 23, 24, 25, 26, 27, 28, 29]. This generalization can be derived from a mesoscopic description based on CTRWs where the reaction term models walkers that are added or removed instantaneously from the system [17, 26]. The mesoscopic description can be motivated by a coarse grained representation of space with diffusion (jumps) between cells and reactions within cells. It is assumed that the waiting time density of jumps is independent of the reaction terms in this description. The characteristic length scale ℓ_D and time scale τ_D in the mesoscopic description are related to physical length scales and physical time scales as follows [30]: (i) $\delta\ell_R \ll \ell_D \ll L$ and (ii) $\delta\tau_D \ll \delta\tau_R \ll \tau_D \ll T$ where $\delta\ell_R$ is the characteristic size of a reaction zone, $\delta\tau_D$ is the characteristic microscopic diffusion time for encounters between reactants, $\delta\tau_R$ is the characteristic microscopic reaction time, L is the size of the domain and T is the time scale of the experiment.

A major difficulty with mesoscopic models for sub-diffusion with reactions, leading to fractional reaction-diffusion equations, is the identification of the particular functional form that should be adopted for particular reaction kinetics. This is especially problematic in the case of nonlinear reaction kinetics. However in the case of linear reaction kinetics the following results have been obtained: If a constant proportion of

walkers are added or removed instantaneously at the start of each step in the CTRW then the reaction term in the corresponding fractional reaction diffusion equation is a linear functional operated on by the same fractional order temporal operator as the diffusion term [30]. If walkers are added or removed at a constant per capita rate over the waiting times between steps then the description as a fractional order reaction-diffusion equation cannot be written simply as a reaction term functional added to the fractional sub-diffusion term [31, 30]. Despite the problems in relating particular reaction kinetics to particular functional forms in nonlinear fractional reaction-diffusion equations it is interesting to investigate such systems as models for pattern formation [18, 32, 28, 29], or front propagation [20, 25], in species undergoing sub-diffusion with nonlinear source and sink terms. Similarly, nonlinear fractional reaction-diffusion equations with fractional order spatial derivatives operating on the diffusion term and with additive reaction terms have been studied as models for pattern formation [33], and front propagation [34], in species undergoing super-diffusion with nonlinear source and sink terms.

One of the best understood models for pattern formation in standard reaction-diffusion systems is Turing instability induced pattern formation [14]. In this model patterning can occur if the homogeneous steady state is linearly stable in the absence of spatial diffusion but linearly unstable in the presence of diffusion. The spatial pattern that results is dominated by the wavelength of the most unstable mode in the linear analysis. In recent work we investigated Turing instability induced pattern formation in a two-species fractional reaction-diffusion system with standard nonlinear activator-inhibitor reaction terms and fractional order temporal derivatives operating on the standard diffusion term [28]. Our theoretical and numerical investigations provided a clear demonstration that the Turing mechanism could account for patterning in this model system. Furthermore it was shown, by lowering the order of the fractional temporal derivative to be the same on both the activator and inhibitor diffusion terms or by having fractional diffusion for the activator but standard diffusion for the inhibitor, that the onset of patterning could occur for lower values of the diffusivity ratios. The dominant wavelength of the spatial patterns that result was also reduced by lowering the order of the fractional temporal derivative.

In this paper we describe our studies of Turing instability induced pattern formation in a two-species fractional reaction-diffusion system with fractional order temporal derivatives operating on both the nonlinear activator and inhibitor reaction terms as well as the diffusion terms. Fractional reaction-diffusion systems with the same fractional order temporal derivative operating on the diffusion terms and the reaction terms have been proposed as models for sub-diffusion with traps [22, 23, 25] and recent numerical studies of pattern formation in systems with fractional order temporal derivatives on diffusion terms and reaction terms were reported in [29]. In the studies reported here we find that the Turing linear instability analysis is again an excellent predictor of both the onset of and the nature of pattern formation. However while the order of the fractional derivative affects the time at which patterns emerge it does not affect the critical diffusivity ratios for the onset of Turing instabilities nor does it affect the

dominant wavelength in the resulting spatial pattern.

The clear difference between the patterning in these different fractional reaction-sub-diffusion equations provides a way of distinguishing which, if either, model might apply in a given experimental situation.

The remainder of this paper is organized as follows. In section 2 we summarize the mescoscopic CTRW formalism that leads to a fractional order temporal derivative operating on a standard Laplacian, combined with an additive reaction term, which may or may not involve fractional temporal derivatives. In section 3 we carry out Turing linear stability analysis in the fractional reaction-diffusion model for the special case in which the same temporal order fractional derivative operates on both the diffusion terms and the reaction terms, and in section 4 we carry out numerical studies of Turing pattern formation in this special case. We discuss our findings further in section 5.

2. Continuous Time Random Walks with Sources and Sinks

The continuous time random walk (CTRW) was introduced by Montroll and Weiss [6], and Scher and Lax [7], as a generalization of the standard random walk introduced by Pearson in 1905 [35]. In the CTRW the waiting times between successive steps and the length of the steps are both random variables with the associated probability density $\Psi(x,t)$ for the particle to step a distance x after waiting a time t. If the walk is considered to take place on a discrete lattice then the conditional probability density $q_n(x,t|x_0,0)$ that a walker starting at x_0 at time zero arrives at position x at time t after n steps, satisfies the recursion equation [7]

$$q_{n+1}(x,t|x_0,0) = \sum_{x'} \int_0^t \Psi(x-x',t-t') q_n(x',t'|x_0,0) dt' \tag{1}$$

where $\Psi(x-x',t-t')$ is the probability density that a random walker jumps a distance $x-x'$, after waiting a time $t-t'$, in a single step. The initial condition that the walker is at x_0 at time zero,

$$q_0(x,t|x_0,0) = \delta_{x,x_0}\delta(t), \tag{2}$$

satisfies the normalization

$$\sum_{x'} \int_0^\infty q_0(x',t'|x_0,0) dt' = 1. \tag{3}$$

If walkers are added and/or removed instantaneously at the start of each step according to a source/sink term $s_n(x,t)$ and if it is assumed that it is assumed that the waiting time distribution of jumps is independent of this addition or removal then the conditional density for walkers to arrive after $n+1$ steps can be written as

$$q_{n+1}(x,t) = \int_0^t \sum_{x'} \left(q_n(x',t') + s_n(x',t')\right) \psi(t-t')\lambda(x-x')\, dt'. \tag{4}$$

The conditional density for walkers to arrive at position x at time t after any number of steps is given by

$$q(x,t|x_0,0) = \sum_{n=0}^{\infty} q_n(x,t|x_0,0). \tag{5}$$

It is convenient to define the net contribution from the source/sink term in a similar manner, as

$$s(x,t) = \sum_{n=0}^{\infty} s_n(x,t). \tag{6}$$

Following [7, 36] we write

$$\sum_{n=0}^{\infty} q_n(x,t|x_0,0) = q_0(x,t|x_0,0) + \sum_{n=0}^{\infty} q_{n+1}(x,t|x_0,0),$$

and then after performing a summation over n, the recursion relation, (4), can be written as

$$q(x,t) = \sum_{x'} \int_0^t \psi(t-t')\lambda(x-x') \left(q(x',t') + s(x',t')\right)\, dt' + \delta(t)\delta_{x,x_0}. \tag{7}$$

In the remainder it is supposed that the probability density $\Psi(x,t)$ decouples in space and time, i.e.,

$$\Psi(x,t) = \psi(t)\lambda(x) \tag{8}$$

where $\psi(t)$ is the waiting time probability density given by

$$\psi(t) = \sum_{x'} \Psi(x',t) \tag{9}$$

and $\lambda(x)$ is the step length probability density given by

$$\lambda(x) = \int_0^{\infty} \Psi(x,t')dt'. \tag{10}$$

It is also useful to define the survival probability distribution $\Phi(t)$ that the walker does not take a step in time interval t

$$\Phi(t) = 1 - \int_0^t \psi(t')dt' = \int_t^{\infty} \psi(t')dt'. \tag{11}$$

The conditional density $p(x,t|x_0,0)$ for walkers to be at position x at time t is equivalent to the density of walkers that arrived at x at earlier times t' and thereafter did not take a step [6, 7, 36], combined now with the walkers introduced or removed by the source/sink term at x at earlier times t', (assuming the same survival characteristics). Thus we can write

$$p(x,t|x_0,0) = \int_0^t \left(q(x,t-t'|x_0,0) + s(x,t-t')\right)\Phi(t')dt'. \tag{12}$$

While it is possible to choose any source term in the above equation the same is not true if $s(x,t)$ models a sink term. Certain choices of the sink term could result in negative

densities. This does not imply that a different model formulation is required for sink terms then for source terms, but rather, judicious selection of the appropriate sink term is required to ensure that particles are not removed from locations at a faster rate then they arrive. The simplest valid choice for a sink term is given by $s(x,t) = -rq(x,t)$ (with $0 < r < 1$). In our mesoscopic formulation this represents the instantaneous removal of a fraction of walkers before they take their next step. The same model equation as (12) with $s(x,t) = -kq(x,t)$ has also been derived as a model for CTRWs with linear degradation [37]. In this derivation the physical interpretation of the parameter k is the probability that a given particle degrades before it takes its next step.

The results in (7) and (12) can be combined using Laplace transforms as follows. The Laplace transform of (12) yields

$$\hat{p}(x,u|x_0,0) = \left(\hat{q}(x,u|x_0,0) + \hat{s}(x,u)\right)\hat{\Phi}(u), \tag{13}$$

and the Laplace transform of (7) yields

$$\hat{q}(x,u|x_0,0) = \sum_{x'}\hat{\Psi}(x',u)\left(\hat{q}(x-x',u|x_0,0) + \hat{s}(x-x',u)\right) + \delta_{x,x_0}. \tag{14}$$

We can combine the results in (13) and (14) to obtain

$$\begin{aligned}\hat{p}(x,u|x_0,0) = &\sum_{x'}\hat{\Psi}(x',u)\hat{\Phi}(u)\left(\hat{q}(x-x',u|x_0,0) + \hat{s}(x-x',u)\right)\\ &+\hat{\Phi}(u)\hat{s}(x,u) + \hat{\Phi}(u)\delta_{x,x_0}, \qquad (15)\\ = &\sum_{x'}\hat{\Psi}(x',u)\hat{p}(x-x',u|x_0,0) + \hat{\Phi}(u)\hat{s}(x,u) + \hat{\Phi}(u)\delta_{x,x_0}. \qquad (16)\end{aligned}$$

The inverse Laplace transform of (16) now yields

$$\begin{aligned}p(x,t|x_0,0) = \Phi(t)\delta_{x,x_0} &+ \sum_{x'}\int_0^t p(x',t'|x_0,0)\Psi(x-x',t-t')dt'\\ &+ \int_0^t \Phi(t-t')s(x,t')\,dt'.\end{aligned} \tag{17}$$

The above equation can be generalized to allow for walkers coming from different starting locations, represented by an initial distribution $c(x_0,0|x_0,0)$ in the density of walkers, as a function of their starting positions $x = x_0$ at time $t = 0$. We can write

$$p(x,t|x_0,0) = \frac{c(x,t|x_0,0)}{c(x_0,0|x_0,0)}$$

so that

$$\begin{aligned}\frac{c(x,t|x_0,0)}{c(x_0,0|x_0,0)} = \Phi(t)\delta_{x,x_0} &+ \sum_{x'}\int_0^t \frac{c(x',t'|x_0,0)}{c(x_0,0|x_0,0)}\Psi(x-x',t-t')dt'\\ &+ \int_0^t \Phi(t-t')s(x,t')\,dt'.\end{aligned} \tag{18}$$

After multiplying by the initial density we obtain,

$$\begin{aligned}c(x,t|x_0,0) = \Phi(t)c(x_0,0|x_0,0)\delta_{x,x_0} &+ \sum_{x'}\int_0^t c(x',t'|x_0,0)\Psi(x-x',t-t')dt'\\ &+ \int_0^t \Phi(t-t')c(x_0,0|x_0,0)s(x,t')\,dt'.\end{aligned} \tag{19}$$

Now we sum over all possible starting points x_0 and define the total density of walkers independent of their starting locations

$$n(x,t) = \sum_{x_0} c(x,t|x_0,0) \tag{20}$$

with initial total density

$$n(x,0) = c(x,0|x,0) \tag{21}$$

and the (renormalized) net contribution from sources and sinks

$$g(x,t) = \sum_{x_0} c(x_0,0|x_0,0)s(x,t), \tag{22}$$

to obtain

$$n(x,t) = \Phi(t)n(x,0) + \sum_{x'} \int_0^t n(x',t')\Psi(x-x',t-t')\,dt' + \int_0^t \Phi(t-t')g(x,t')\,dt'. \tag{23}$$

The above equation can also be motivated by heuristic arguments [17, 20, 26]. The additional source/sink term $\int_0^t \Phi(t-t')g(x,t')\,dt'$ represents the net contribution to the density of walkers at x and t due to i) walkers instantaneously added at x at time $t' < t$ that then do not jump from x over the time $(t-t')$ and ii) walkers instantaneously removed at x at time $t' < t$ that would not otherwise have jumped from x during the time $(t-t')$. Thus walkers with survival characteristics represented through $\Phi(t)$ are added or removed from the system at a rate $g(x,t)$. The formulation of the problem in Eq.(23) is a general model for the instantaneous addition or removal of walkers in a mesoscopic description but there would need to be careful consideration of the appropriate choice for $g(x,t)$ to model a particular physical process. This is particularly true if $g(x,t)$ represents a sink, since some choices (including a simple linear functional of $n(x,t)$) could lead to unphysical negative solutions [30].

The long time asymptotic behaviour of $n(x,t)$ that is consistent with (23) can be described by a fractional reaction diffusion equation [17]. The steps are as follows; carry out a spatial Fourier transform and a temporal Laplace transform, use asymptotic expansions in small values of the Fourier and Laplace variables, re-formulate the inverse transforms using the definition of the Riemann-Liouville fractional derivative. Explicitly, the Fourier-Laplace transform of (23) with Fourier variable q and Laplace variable u yields

$$\hat{\hat{n}}(q,u) = \hat{\Phi}(u)\hat{n}(q,0) + \hat{\psi}(u)\hat{\lambda}(q)\hat{\hat{n}}(q,u) + \hat{\Phi}(u)\hat{n}(q,0) + \hat{\Phi}(u)\hat{\hat{g}}(q,u) \tag{24}$$

The Laplace transform of the survival probability, (11), can be written as

$$\hat{\Phi}(u) = \frac{1}{u} - \frac{\hat{\psi}(u)}{u} \tag{25}$$

and the small q asymptotic expansion of the step length density is given by

$$\hat{\lambda}(q) \sim 1 - \frac{q^2\sigma^2}{2} + O(q^4) \tag{26}$$

with

$$\sigma^2 = \int r^2 \lambda(r)\, dr \tag{27}$$

finite. We can thus write (24) as

$$u\hat{\hat{n}}(q,u) \approx \left(1-\hat{\psi}(u)\right)\hat{n}(q,0) + u\hat{\psi}(u)\left(1-\frac{q^2\sigma^2}{2}\right)\hat{\hat{n}}(q,u) + \left(1-\hat{\psi}(u)\right)\hat{\hat{g}}(q,u). \tag{28}$$

We now consider asymptotic small u results for a heavy tailed waiting time density

$$\psi(t) \sim \frac{K}{\tau^\alpha} t^{-\alpha-1} \tag{29}$$

that is characteristic of anomalous sub-diffusion (see e.g., [8]). The asymptotic Laplace transform for this density function is obtained from a Tauberian (Abelian) theorem [38, 39] as

$$\hat{\psi}(u) \sim 1 - \frac{K\Gamma(1-\alpha)\tau^\alpha}{\alpha} u^\alpha. \tag{30}$$

Note that a similar expression for the Laplace transform of the waiting time density results without the need for long time asymptotics in the special case where the waiting time density is given by the derivative of a Mittag-Leffler function [40]. We now substitute the above expansion, (30), into (28) to arrive at

$$u\hat{\hat{n}}(q,u) \approx \frac{K\Gamma(1-\alpha)\tau^\alpha}{\alpha} u^\alpha \hat{n}(q,0) + u\left(1-\frac{K\Gamma(1-\alpha)\tau^\alpha}{\alpha}u^\alpha\right)\left(1-\frac{q^2\sigma^2}{2}\right)\hat{\hat{n}}(q,u) + \frac{K\Gamma(1-\alpha)\tau^\alpha}{\alpha} u^\alpha \hat{\hat{g}}(q,u) \tag{31}$$

If we re-arrange this equation and retain only leading order terms then

$$u\hat{\hat{n}}(q,u) - \hat{n}(q,0) \approx -\frac{\alpha}{K\Gamma(1-\alpha)\tau^\alpha} u^{1-\alpha} \frac{q^2\sigma^2}{2}\hat{\hat{n}}(q,u) + \hat{\hat{g}}(q,u). \tag{32}$$

The inverse Laplace transform and inverse Fourier transform of (32) now yields the asymptotic approximation

$$\frac{\partial n}{\partial t} = D(\alpha)\mathcal{D}^{1-\alpha}\left[\frac{\partial^2 n}{\partial x^2}\right] + g(x,t) \tag{33}$$

where

$$D(\alpha) = \frac{\sigma^2\alpha}{2K\Gamma(1-\alpha)\tau^\alpha}. \tag{34}$$

Here we use the notation

$$\mathcal{D}^{1-\alpha}\left[y(x,t)\right] = \frac{\partial^{1-\alpha}}{\partial t^{1-\alpha}} y(x,t) + \mathcal{L}^{-1}\{\frac{\partial^{-\alpha}}{\partial t^{-\alpha}} y(x,t)|_{t=0}\}, \qquad 0<\alpha<1 \tag{35}$$

where

$$\frac{\partial^{1-\alpha}}{\partial t^{1-\alpha}} y(x,t) \tag{36}$$

is the Riemann-Liouville fractional derivative defined as the ordinary derivative of the Riemann-Liouville fractional integral

$$\mathcal{D}^{-\alpha}\left[y(x,t)\right] = \frac{\partial^{-\alpha}}{\partial t^{-\alpha}} y(x,t) = \frac{1}{\Gamma(\alpha)} \int_0^t \frac{y(x,t)}{(t-s)^{1-\alpha}}\, ds, \qquad 0 < \alpha < 1. \tag{37}$$

Note that the operator $\mathcal{D}^{\gamma}$ has a different definition depending on whether γ is positive, (35), or negative, (37). Note too that the inverse Laplace transform of the fractional integral evaluated at time zero, which appears in the operator $\mathcal{D}^{1-\alpha}$ in (35), will cancel in (33) if the method of Laplace transforms is applied to find the solution.

The fractional reaction-diffusion equation, (33), as written, has a fractional order temporal derivative operating on the diffusion term but no explicit fractional order temporal derivative operating on the the source/sink reaction term. However the source/sink term has not been related to any particular reaction kinetics in the derivation above and indeed this is still an outstanding problem [30]. Two *ad hoc* source/sink terms that have been considered in reaction sub-diffusion problems are [17, 18, 20, 24, 30]

$$g(x,t) = f(n(x,t)), \tag{38}$$

and [25, 29]

$$g(x,t) = \frac{\partial^{1-\alpha}}{\partial t^{1-\alpha}} f(n(x,t)) \tag{39}$$

where $f(n(x,t))$ is the standard functional for reaction rate kinetics described by the law of mass action. The utility of either of these models as an approximation of the long time behaviour in physical processes driven by reaction with sub-diffusion is yet to be tested by comparison with physical experiments.

In earlier work we investigated Turing instability induced pattern formation in a two-species fractional reaction sub-diffusion equation, with reaction terms from the law of mass action for activator-inhibitor systems, and with a fractional order temporal derivative operating on the diffusion term, i.e., a two-species variant of (33) and (38). We now consider Turing instability induced pattern formation in a two-species fractional reaction sub-diffusion equation, with a fractional order temporal derivative operating on both the reaction terms from the law of mass action for activator-inhibitor systems, and on the diffusion term. ie., a two-species variant of (33) and (39).

Before we leave this section it is worth noting the following: A fractional reaction sub-diffusion equation with temporal order derivatives operating explicitly on the source/sink term as well the diffusion term can be obtained if the survival probability for walkers added or removed by the source/sink term is taken to be a standard Poisson distribution rather than a heavy tailed distribution. Furthermore if a constant proportion, r, of walkers are added or removed instantaneously at the start of each step then the corresponding source/sink term in (33) is given by the fractional temporal derivative of a linear functional [30]

$$g(x,t) = \frac{r-1}{r} \frac{\alpha}{K\Gamma(1-\alpha)\tau^{\alpha}} \mathcal{D}^{1-\alpha} n. \tag{40}$$

As a physical example, the diffusion of degrading morphogens in a microscopically heterogeneous extracellular environment, which has recently been modelled using CTRWs [37], can be modelled using a reaction sub-diffusion equation with temporal order derivatives operating on both the Laplacian diffusion term and a linear sink term [30]. The extension to nonlinear reaction terms is non-trivial but *ad hoc* models with temporal order derivatives operating on both the Laplacian diffusion term and nonlinear reaction kinetics from the law of mass action have been considered by other authors [25, 29], and results for front propagation have been found to be in reasonable agreement with Monte Carlo simulations [25].

3. Turing Instability Analysis

We now consider the stability of the homogeneous steady state solutions in two-species fractional reaction-diffusion equations where the same temporal order derivative operates on both the diffusion terms and the reaction terms. If both species have similar diffusive properties then the general form of the two-species fractional reaction-diffusion model in one spatial dimension in this special case is

$$\frac{\partial n_1(x,t)}{\partial t} = \mathcal{D}^{1-\gamma}\left[\lambda f_1(n_1,n_2) + \frac{\partial^2 n_1}{\partial x^2}\right], \tag{41}$$

$$\frac{\partial n_2(x,t)}{\partial t} = \mathcal{D}^{1-\gamma}\left[\lambda f_2(n_1,n_2) + d\frac{\partial^2 n_2}{\partial x^2}\right]. \tag{42}$$

In these equations, $n_1(x,t)$ and $n_2(x,t)$ are the number densities for the two species, f_1 and f_2 are (generally nonlinear) functions describing the reaction kinetics, d is the ratio of the diffusion coefficients of species 2 to species 1, γ in the range $0 < \gamma \leq 1$ is the fractional exponent and $\lambda > 0$ is a scaling variable which can be interpreted as the linear size of the spatial domain, or as the relative strength of the reaction terms. In this model, species 1 is an activator of species 2, which is an inhibitor of species 1. The fractional reaction-diffusion system in (41), (42) can be re-written with Caputo fractional temporal derivatives operating on the left hand side and no (fractional order) temporal derivatives operating on the Laplacian terms or the reaction terms. The fractional order temporal derivatives affect the growth rates of linearized spatial modes in both representations and must be considered in Turing instability analysis. As canonical examples of reaction kinetics we consider both Brusselator reaction kinetics [41]

$$f_1(n_1,n_2) = 2 - 3n_1 + n_1^2 n_2 \tag{43}$$

$$f_2(n_1,n_2) = 2n_1 - n_1^2 n_2 \tag{44}$$

and Gierer-Meinhardt reaction kinetics [42]

$$f_1(n_1,n_2) = 1 - n_1 + 3\frac{n_1^2}{n_2} \tag{45}$$

$$f_2(n_1,n_2) = n_1^2 - n_2. \tag{46}$$

For each model we consider the one-dimensional domain $0 \leq x \leq L$ with zero-flux boundary conditions at both ends, i.e.,

$$\left.\frac{\partial n_j}{\partial x}\right|_{x=0} = \left.\frac{\partial n_j}{\partial x}\right|_{x=L} = 0, \qquad j = 1, 2. \tag{47}$$

Linearizing the model equations, (41) and (42), around the homogeneous steady state (n_1^*, n_2^*) we obtain the evolution equations for the perturbations Δn_j as follows:

$$\frac{\partial \Delta n_1(x,t)}{\partial t} = \mathcal{D}^{1-\gamma}\left[\lambda\left(a_{11}\Delta n_1 + a_{12}\Delta n_2\right) + \frac{\partial^2 \Delta n_1}{\partial x^2}\right], \tag{48}$$

$$\frac{\partial \Delta n_2(x,t)}{\partial t} = \mathcal{D}^{1-\gamma}\left[\left[\lambda\left(a_{21}\Delta n_1 + a_{22}\Delta n_2\right) + d\frac{\partial^2 \Delta n_2}{\partial x^2}\right]\right. \tag{49}$$

where the coefficients

$$a_{ij} = \left.\frac{\partial f_i}{\partial x_j}\right|_{(n_1^*, n_2^*)}, \qquad i = 1, 2, \quad j = 1, 2.$$

In earlier work [18] we showed that Turing instabilities in linear fractional reaction diffusion systems could readily be identified after taking a temporal Laplace transform and a spatial Fourier transform. If we apply a temporal Laplace transform (variable u) and a spatial Fourier transform (variable q) to the linearised equations, (48) and (49), (or to a linearization of the Caputo representation with fractional temporal derivatives on the left hand side of the equations only) and solve for the transformed perturbations we find

$$\hat{\Delta\hat{n}}_1(q,u) = \frac{\left(u^\gamma + q^2 d - \lambda a_{22}\right)\hat{\Delta n}_1(q,0) + \lambda a_{12}\hat{\Delta n}_2(q,0)}{u^{1-\gamma}\left[\left(u^\gamma + q^2 - \lambda a_{11}\right)\left(u^\gamma + q^2 d - \lambda a_{22}\right) - \lambda^2 a_{12}a_{21}\right]} \tag{50}$$

$$\hat{\Delta\hat{n}}_2(q,u) = \frac{\lambda a_{21}\hat{\Delta n}_1(q,0) + \left(u^\gamma + q^2 - \lambda a_{11}\right)\hat{\Delta n}_2(q,0)}{u^{1-\gamma}\left[\left(u^\gamma + q^2 - \lambda a_{11}\right)\left(u^\gamma + q^2 d - \lambda a_{22}\right) - \lambda^2 a_{12}a_{21}\right]} \tag{51}$$

where $\hat{\Delta n}_1(q,0)$ and $\hat{\Delta n}_2(q,0)$ are determined by the initial conditions. The conditions for Turing instabilities can now be found by considering the large t asymptotic behaviour in the inverse Laplace transforms

$$\hat{\Delta n}_j(q,t) = \frac{1}{2\pi i}\int_{c-i\infty}^{c+i\infty} \hat{\Delta\hat{n}}_j(q,u)e^{ut}\,du. \tag{52}$$

In general, this asymptotic behaviour can be deduced by applying the Cauchy residue theorem considering a modified Bromwich contour with a branch cut from the branch point at $u = 0$ along the negative real axis [18]. The unstable wavenumbers q are identified as the q values for which the real part of the poles $u^\star(q)$ of $\hat{\Delta\hat{n}}_j(q,u)$ are positive. In the present case the inverse Laplace transforms can be evaluated explicitly in terms of Mittag-Leffler functions and the instability conditions can be deduced from known asymptotic properties of these functions. We follow this latter approach here. First we note that the term inside the square brackets in the denominator of $\hat{\Delta\hat{n}}_j(q,u)$ is a quadratic

$$\left(s + q^2 - \lambda a_{11}\right)\left(s + q^2 d - \lambda a_{22}\right) - \lambda^2 a_{12}a_{21} \tag{53}$$

in the variable $s = u^\gamma$. We denote the zeroes of this quadratic by $s^+(q)$ and $s^-(q)$ where

$$s^{\pm}(q) = -\frac{1}{2}\left[q^2\left(d+1\right) - \lambda\left(a_{11}+a_{22}\right)\right] \pm \sqrt{\frac{1}{4}\left[q^2\left(d+1\right) - \lambda\left(a_{11}+a_{22}\right)\right]^2 - \left[\left(q^2-\lambda a_{11}\right)\left(dq^2-\lambda a_{22}\right) - \lambda^2 a_{12}a_{21}\right]}. \tag{54}$$

The expressions for the inverse Laplace transforms have different functional forms depending on the whether the zeroes are real and distinct, real and repeated, or complex conjugate pairs as follows:

3.1. Real distinct zeroes

In this case we can write

$$\hat{\Delta\hat{n}}_j(q,s) = \left(\frac{\alpha_j\left(s^+(q),q\right)}{s^+(q)-s^-(q)}\right)\left(\frac{u^{\gamma-1}}{u^\gamma - s^+(q)}\right) - \left(\frac{\alpha_j\left(s^-(q),q\right)}{s^+(q)-s^-(q)}\right)\left(\frac{u^{\gamma-1}}{u^\gamma - s^-(q)}\right) \tag{55}$$

where the functions $\alpha_j(s,q)$ are given by

$$\alpha_1\left(s,q\right) = \left(s+q^2d-\lambda a_{22}\right)\hat{\Delta n}_1(q,0) + \lambda a_{12}\hat{\Delta n}_2(q,0) \tag{56}$$

$$\alpha_2\left(s,q\right) = \lambda a_{21}\hat{\Delta n}_1(q,0) + \left(s+q^2-\lambda a_{11}\right)\hat{\Delta n}_2(q,0). \tag{57}$$

The temporal behaviour of the transform in (55) can now be found by inverting the Laplace transform to give

$$\hat{\Delta n}_j(q,t) = \frac{\alpha_j\left(s^+(q),q\right)}{s^+(q)-s^-(q)}E_\gamma\left(s^+(q)t^\gamma\right) - \frac{\alpha_j\left(s^-(q),q\right)}{s^+(q)-s^-(q)}E_\gamma\left(s^-(q)t^\gamma\right) \tag{58}$$

where $E_\gamma(z)$ is the Mittag-Leffler function in one parameter [43] with asymptotic properties [44, 45, 46]

$$E_\gamma(z) \sim \frac{1}{\gamma}e^{z^{\frac{1}{\gamma}}} - \sum_{k=1}^{\infty}\frac{z^{-k}}{\Gamma(1-\gamma k)} \qquad \text{as} \quad z\to\infty \tag{59}$$

and

$$E_\gamma(z) \sim -\sum_{k=1}^{\infty}\frac{z^{-k}}{\Gamma(1-\gamma k)} \qquad \text{as} \quad z\to-\infty. \tag{60}$$

That is, the Mittag-Leffler function decays to zero for large negative values of its argument but goes to infinity for large positive values. It follows that if both $s^+(q)$ and $s^-(q)$ are negative for a range of q values then the Mittag-Leffler function will decay with time for those q values and thus perturbations of these wave numbers will decay to zero. If this occurs for all values of q then no Turing pattern will form. Alternatively if $s^+(q)$ is positive for some q values ($s^-(q)$ is always negative in this case) then the term in the perturbation, involving $s^+(q)$, will grow with time and a Turing pattern will form.

3.2. Real repeated zeroes

In this case we write $s^+ = s^- = s^*$ say and then

$$\hat{\Delta\hat{n}}_j(q,s) = \alpha_j\left(s^*(q),q\right)\frac{u^{\gamma-1}}{\left(u^\gamma - s^*(q)\right)^2} + \hat{\Delta n}_j(q,0)\frac{u^{\gamma-1}}{u^\gamma - s^*(q)}. \tag{61}$$

The inverse Laplace transform now yields

$$\hat{\Delta n}_j(q,t) = \alpha_j\left(s^*(q),q\right)t^\gamma E_\gamma^{(1)}\left(s^*(q)t^\gamma\right) + \hat{\Delta n}_j(q,0)E_\gamma\left(s^*(q)t^\gamma\right). \tag{62}$$

where $E_\gamma^{(1)}(z)$ is the first derivative of the Mittag-Leffler function in one parameter [43]. Since the repeated zeroes of (53) are negative, it follows from the asymptotic result in (60) together with the asymptotic result

$$E_\gamma^{(1)}(-z) \sim \sum_{p=1}^{\infty}\frac{p(-z)^{-(p+1)}}{\Gamma(1-\gamma p)} \qquad \text{as} \quad z\to-\infty$$

that modes with wave numbers for which $s^+(q) = s^-(q)$ will decay to zero, and no Turing pattern will form.

3.3. Complex conjugate pair of zeroes

In this case we write the zeroes as

$$s^\pm = a \pm ib$$

where a, b are both real. The Laplace transforms can now be written in the form

$$\begin{aligned}\hat{\Delta\hat{n}}_j(q,u) = \alpha_j\left(a(q),q\right)&\sum_{n=0}^{\infty}(-1)^n\left(b(q)\right)^{2n}\frac{u^{\gamma-1}}{\left(u^\gamma - a(q)\right)^{2n+2}}\\ &+ h_j(q)\sum_{n=0}^{\infty}(-1)^n\left(b(q)\right)^{2n}\frac{u^{\gamma-1}}{\left(u^\gamma - a(q)\right)^{2n+1}},\end{aligned} \tag{63}$$

which can be inverted to yield

$$\begin{aligned}\hat{\Delta n}_j(q,t) = \alpha_j\left(a(q),q\right)&\sum_{n=0}^{\infty}\frac{(-1)^n\left(b(q)\right)^{2n}}{(2n+1)!}t^{(2n+1)\gamma}E_\gamma^{(2n+1)}\left(a(q)t^\gamma\right)\\ &+ \hat{\Delta n}_j(q,0)\sum_{n=0}^{\infty}\frac{(-1)^n\left(b(q)\right)^{2n}}{(2n)!}t^{(2n)\gamma}E_\gamma^{(2n)}\left(a(q)t^\gamma\right)\end{aligned} \tag{64}$$

where, $E_\gamma^{(k)}(z)$, is the k^{th} derivative of the Mittag-Leffler function $E_\gamma(z)$. A more convenient expression for ascertaining the asymptotic behaviour can be found by first writing

$$\hat{\Delta\hat{n}}_j(q,u) = \frac{\alpha_j\left(s^+(q),q\right)}{2ib(q)}\frac{u^{\gamma-1}}{u^\gamma - s^+(q)} - \frac{\alpha_j\left(s^-(q),q\right)}{2ib(q)}\frac{u^{\gamma-1}}{u^\gamma - s^-(q)} \tag{65}$$

and then inverting to find

$$\hat{\Delta n}_j(q,t) = \frac{\alpha_j\left(s^+(q),q\right)}{2ib(q)}E_\gamma\left(s^+(q)t^\gamma\right) - \frac{\alpha_j\left(s^-(q),q\right)}{2ib(q)}E_\gamma\left(s^-(q)t^\gamma\right). \tag{66}$$

This equation is similar to the expression given in (58) except the arguments of the Mittag-Leffler functions are now complex. The result given in (60) still holds provided $|\arg(-z)| < (1-\gamma/2)\,\pi$ as $|z| \to \infty$ [44]. For γ values in the interval $0 < \gamma \leq 1$ this criterion is satisfied by complex numbers with $\Re(z) \leq 0$. Hence the wavenumbers, q, corresponding to complex zeroes, will decay to zero, and no Turing pattern will form. This can readily be seen in the case of standard diffusion, $\gamma = 1$, where $\Delta\hat{n}_j(q,t)$ can be simplified to

$$\Delta\hat{n}_j(q,t) = \alpha_j\left(a(q),q\right)e^{at}\cos\left(bt\right) + \frac{\Delta\hat{n}_j(q,0)}{b}e^{at}\sin\left(bt\right) \tag{67}$$

which decays to zero for $a < 0$.

3.4. Critical d

In the preceding analysis we found that the condition for a Turing instability in the model system described by (41) and (42) can be expressed by the single condition that $u^+(q)$ is real and positive for some non-zero values of q. It follows from (54) that this condition is met if

$$M(q^2) = (q^2 - \lambda a_{11})(dq^2 - \lambda a_{22}) - \lambda^2 a_{21}a_{12} < 0 \tag{68}$$

for some $q \neq 0$. The function $M(q^2)$ is a quadratic function of q^2 with a single minimum at

$$q^{\star 2} = \frac{\lambda d a_{11} + \lambda a_{22}}{2d}. \tag{69}$$

Thus if $M(q^{\star 2}) < 0$ then $M(q^2)$ will be negative for a range of non-zero q as required. If we define the stability matrix

$$\mathbf{A} = \begin{pmatrix} a_{11} & a_{12} \\ a_{21} & a_{22} \end{pmatrix} \tag{70}$$

then the condition that $M(q^{\star 2}) < 0$ leads to

$$(a_{22} + d a_{11})^2 > 4d(\det \mathbf{A}) \tag{71}$$

which is satisfied if

$$d > d^\star = \left(\frac{1}{a_{11}}\left[\sqrt{\det \mathbf{A}} + \sqrt{-a_{12}a_{21}}\right]\right)^2 \tag{72}$$

and then the range of excited q values is defined by

$$\begin{aligned} -\sqrt{(da_{11}+a_{22})^2 - 4d(\det\mathbf{A})} \\ \leq 2dq^2 - (da_{11}+a_{22}) \\ \leq +\sqrt{(da_{11}+a_{22})^2 - 4d(\det\mathbf{A})}. \end{aligned} \tag{73}$$

The critical value of d defined by (72) and the range of excited modes defined by (73) are exactly the same as for the standard reaction-diffusion equation [14]. In the case of Gierer-Meinhardt reaction kinetics and Brusselator reaction kinetics the critical d values are $d^* = 10 + 4\sqrt{6} \approx 19.7980$ and $d^* = 12 + 8\sqrt{2} \approx 23.2127$, respectively.

3.5. Approach to steady state

Although the pattern of excited modes in the fractional system considered here is the same as the corresponding standard case, the temporal evolution of the transforms $\Delta\hat{n}_1(q,t)$ and $\Delta\hat{n}_2(q,t)$, given in (58) is determined by Mittag-Leffler functions of t^γ and hence we anticipate that the initial growth of the modes will be slowed for $\gamma < 1$. Indeed it can be shown through rescaling analysis that even in the fully nonlinear system the approach to the non-homogeneous steady state (assuming such a state exists) is governed by a pure function of t^γ. To see this we introduce a change of variables $z = t^\gamma$ and $n_j(x,t) = g_j(x,z) = g_j(x,t^\gamma)$ into (41) and (42). The bracketed terms on the right hand side can now be written as $p_j(x,z) = p_j(x,t^\gamma)$. We now use the chain rule to write

$$\frac{\partial n_j(x,t)}{\partial t} = \gamma t^{\gamma-1}\frac{\partial g_j(x,z)}{\partial z}. \tag{74}$$

In terms of our transformed variables we can also write (See Appendix)

$$\frac{\partial^{1-\gamma}}{\partial t^{1-\gamma}}p_j(x,t^\gamma) = \gamma t^{\gamma-1}\frac{1}{\gamma}\left(P^{\gamma,1-\gamma}_{-\frac{1}{\gamma}}p_j(x,z)\right)(z) \tag{75}$$

where

$$\left(P^{\tau,\alpha}_{\beta}r\right)(z) = \prod_{j=0}^{\eta-1}\left(\tau + j - \frac{1}{\beta}z\frac{d}{dz}\right)\left(K^{\tau+\alpha,\eta-\alpha}_{\beta}r\right)(z) \tag{76}$$

is the Erdelyi-Kober fractional derivative operator with $\eta - 1 < \alpha \leq \eta$ and η being a natural number [47].

It now follows that the fractional reaction diffusion equations, (41) and (42), can be written in transformed variables as

$$\frac{\partial g_j(x,z)}{\partial z} = \frac{1}{\gamma}\left(P^{\gamma,1-\gamma}_{-\frac{1}{\gamma}}p_j(x,z)\right)(z) \tag{77}$$

which is a governing equation solely in terms of x and z showing that the solution

$$n_j(x,t) = g_j(x,z) = g_j(x,t^\gamma) \tag{78}$$

is a pure function of x and t^γ. Whilst we have shown in (77) that the approach to the steady state is a function of t^γ it should be noted that the equation is still parameterized by the fractional exponent. This can be seen in the Turing instability analysis in (58), (62) and (66), where (in the linear case) the temporal evolution of the modes is expressed as an explicit function of t^γ through the Mittag-Leffler functions. However the Mittag-Leffler functions are still parameterized by the fractional exponent and they only reduce to the solution in the standard case when the frational exponent is one. Thus in order to gauge the accuracy of the Turing stability analysis results, as a reliable predictor of Turing pattern formation, we are required to run simulations for each value of the fractional exponent.

4. Numerical simulations

The fractional reaction diffusion systems with both Brusselator and Gierer-Meinhardt reaction kinetics were simulated using an implicit finite difference scheme similar to that described in Henry, Langlands and Wearne [28]. The model equations were discretized using finite differences with a backward time step for the time derivative and a centred difference approximation for the spatial derivative. The fractional derivative of order $1-\gamma$ with respect to time at $t = t_k$ was approximated using the L1 scheme [48]

$$\frac{d^{1-\gamma}y}{dt^{1-\gamma}} \approx \frac{\Delta t^{\gamma-1}}{\Gamma(1+\gamma)} \left\{ \frac{\gamma y(0)}{k^{1-\gamma}} + \sum_{l=1}^{k} \left(y\left(t_{l+1}\right) - y\left(t_l\right)\right) \left((k-l+1)^{\gamma} - (k-l)^{\gamma}\right) \right\}$$

where Δt is the step length in time and $\Gamma(x)$ is the Gamma function. In our simulations we have retained the full evaluation of the sum for the computation of the fractional derivative. This improves accuracy at the expense of increased computation.

We denote the solution of species n_j at time $t = j\Delta t$ and position $x = i\Delta x$ by

$$n_j\left(i\Delta x, k\Delta t\right) = n_{j,i}^{k}.$$

The finite difference equations are for $i = 2, \ldots, N-1$ and $j = 1, 2$

$$\begin{aligned} & n_{j,i}^{k+1}\left(1+2\delta_j\right) - \delta_j n_{j,i-1}^{k+1} - \delta_j n_{j,i+1}^{k+1} - \delta_{fj} f_j\left(n_{1,i}^{k+1}, n_{2,i}^{k+1}\right) \\ & = n_{j,i}^{k} + \delta_{fj}\left(g_{j,i}^{(l)}\omega_j^k + \sum_{l=2}^{k} \beta_{k-l+2} g_{j,i}^{(l)}\right) \end{aligned} \tag{79}$$

where

$$\begin{aligned} & g_{j,i}^{(k)} = d_j \nabla n_{j,i}^{k} + f_j\left(n_{1,i}^{k}, n_{2,i}^{k}\right), \\ & \nabla n_{j,i}^{k} = n_{j,i+1}^{k} - 2n_{j,i}^{k} + n_{j,i-1}^{k}, \\ & \delta_{fj} = \frac{\Delta t^{\gamma_j}}{\Delta x^2 \Gamma(1+\gamma_j)}, \\ & \delta_j = d_j \delta_{fj}, \end{aligned} \tag{80}$$

and $d_1 = 1$ and $d_2 = d$. For the boundary point, $i = 1$, the value of $n_{j,i-1}^{k}$ in (79) and (80) is replaced by $n_{j,2}^{k}$. Likewise the value of $n_{j,i+1}^{k}$ is replaced by $n_{j,N-1}^{k}$ at the boundary point $i = N$.

The weights of the fractional derivative in (79) are given by

$$\omega_j^k = \frac{\gamma_j}{k^{1-\gamma_j}} - \left[k^{\gamma_j} - (k-1)^{\gamma_j}\right]$$

and

$$\beta_s = s^{\gamma_j} - 2\left(s-1\right)^{\gamma_j} + \left(s-2\right)^{\gamma_j} \quad s = 2, 3, \ldots, k.$$

The "constant" terms of the sum are given on the right of these equations. In recent work [49] we showed that the implicit scheme for the fractional diffusion equation with temporal order derivative $1-\gamma$ operating on the diffusion term is unconditionally stable with accuracy $O(\Delta x^2)$ in the spatial grid size and $O(\Delta t^{1+\gamma})$ in the fractional time step.

We have carried out simulations based on the above scheme with spatial grid spacing $\Delta x = 100/255$ and with $\Delta t = 1/100$ for 15000 time steps and for a range of $\gamma = 0.1, 0.2, 0.3, \ldots, 0.9, 1.0$. In our simulations we have investigated both random and sinusoidal initial perturbations between -10^{-2} and $+10^{-2}$ from the homogeneous steady state. Surface profiles and surface density plots of the activator $n_1(x,t)$ from some of the simulations are shown for Gierer-Meinhardt reaction kinetics with $d = 20$ (Figure 1) and for Brusselator reaction kinetics with $d = 25$ (Figure 2). In the surface density plots $n_1(x,t) \geq n_1^\star$ is shown as black and $n_1(x,t) < n_1^\star$ is shown as white.

There are several features to note from the simulations: (i) There are no complex spatio-temporal patterns similar to those that we reported recently (see especially Figure 4 and Figure 5 in [28]) for fractional activator-inhibitor systems with the temporal fractional order derivative operating on the diffusion term but not the reaction term. (ii) The patterns appear to evolve to the same final steady state. This final steady state is evident in simulations with $\gamma = 1.0, 0.9, 0.8$ in the fractional Gierer-Meinhardt model (see Fig.1(a) for $\gamma = 0.8$) and $\gamma = 1.0, 0.9, 0.8, 0.7$ in the fractional Brusselator model (see Fig.2(a) for $\gamma = 0.8$) but the steady state can only be inferred for lower values of γ. (iii) The time taken to approach the steady state increases with decreasing γ. This relaxation time is a manifestation of the temporal memory of the initial state embodied in the fractional temporal derivative. Simulations with different initial conditions reveal that the memory of the initial conditions is also evident in the spatial patterns in the transient relaxation regime. (v) Turing linear stability analysis is an excellent predictor of spatial pattern formation in fractional reaction-diffusion systems.

In order to further investigate the growth of unstable modes as a function of the parameter γ we have recorded the time for the maximum perturbation away from the steady state in our simulations to increase to a nominal value of 10^{-2}. The deviation from the steady state decreases initially but then proceeds to grow. The time for the maximum perturbation to reach the value of 10^{-2} is measured in this growth regime. A plot of the logarithm of this time versus $1/\gamma$ is shown in Figure 3 for the Brusselator model. Note that only results for $\gamma \geq 0.5$ are shown as the perturbation remained below 10^{-2} in the simulated time period for $\gamma \leq 0.4$. The linear behaviour in Figure 3 is consistent with the Fourier transform results for the time evolution of the perturbations in (58) based on linear stability analysis. The time evolution of the maximal displacement should follow that of the maximally excited mode and from (58) this is given by

$$\hat{\Delta n}_j(t) = A_j E_\gamma \left(s^+(q^\star) t^\gamma \right) \tag{81}$$

where $q^\star$ is defined by (69). If we use the asymptotic result in (59) then in the growth regime we have

$$\hat{\Delta n}(t) \sim \frac{A}{\gamma} \exp(s^+(q^\star)^{\frac{1}{\gamma}}\, t). \tag{82}$$

Thus if we let τ denote the time with displacement $\hat{\Delta n}(\tau) = \hat{\Delta n}^\star$ then after taking

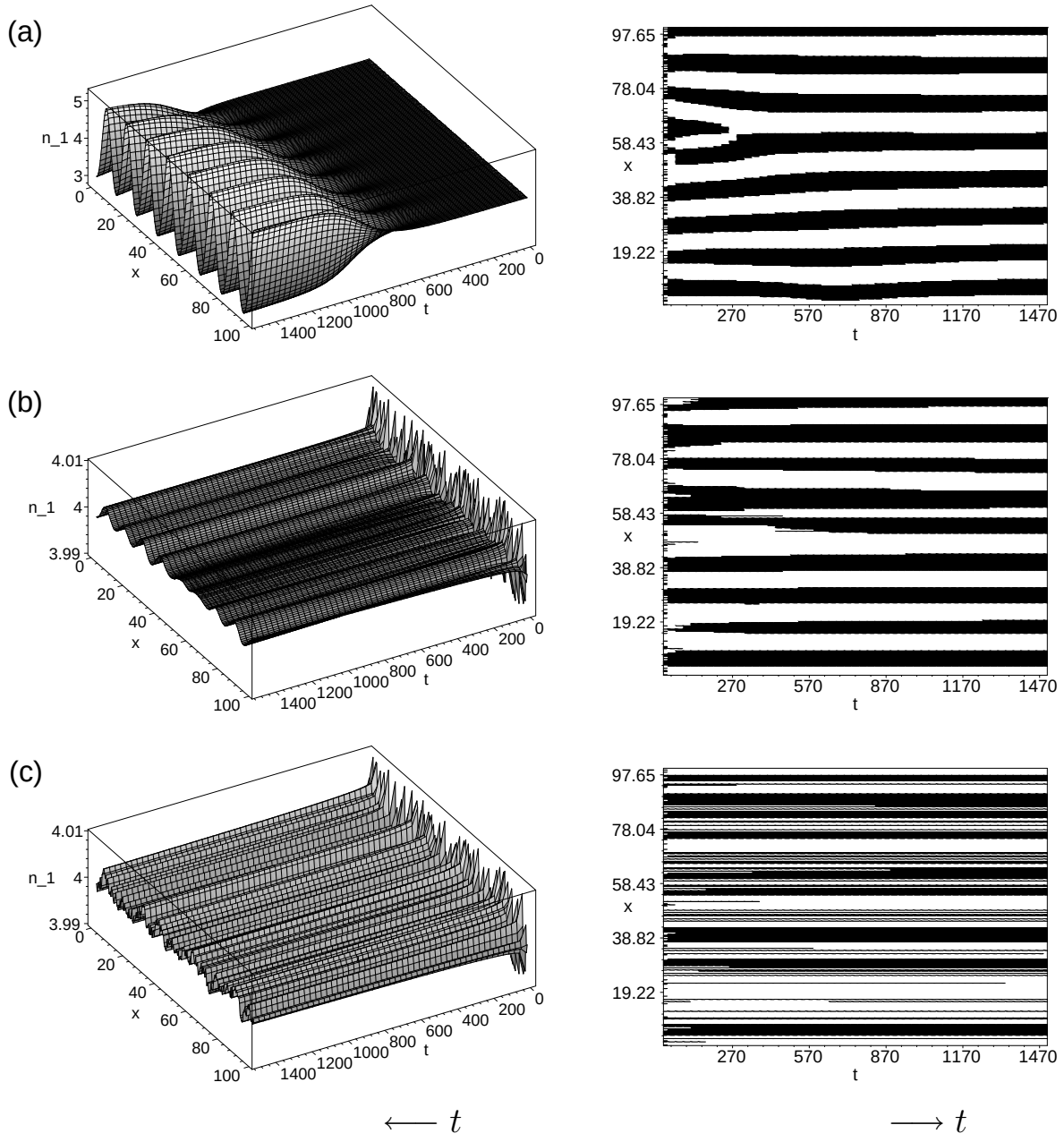

Figure 1. Surface profiles and surface density plots for $n_1(x,t)$ in the fractional Gierer-Meinhardt model with randomly perturbed initial conditions and $d = 20$: (a) $\gamma = 0.8$; (b) $\gamma = 0.5$; (c) $\gamma = 0.2$.

logarithms of both sides in (82) we have

$$\ln \tau \sim -\frac{1}{\gamma} \ln \left(s^{+}(q^{\star}) \right) + \ln \left(\frac{\hat{\Delta n}^{\star}}{\hat{\Delta n}_0} \right) \tag{83}$$

where $\hat{\Delta n}_0$ is the displacement at the start of the growth regime. In the case of the Brusselator reaction kinetics we have $a_{11} = 1$, $a_{12} = 4$, $a_{21} = -2$, $a_{22} = -4$ and $q^{\star} = [(d-4)/(2d)]^{1/2}$ so that if we substitute these values together with $d = 25$ into

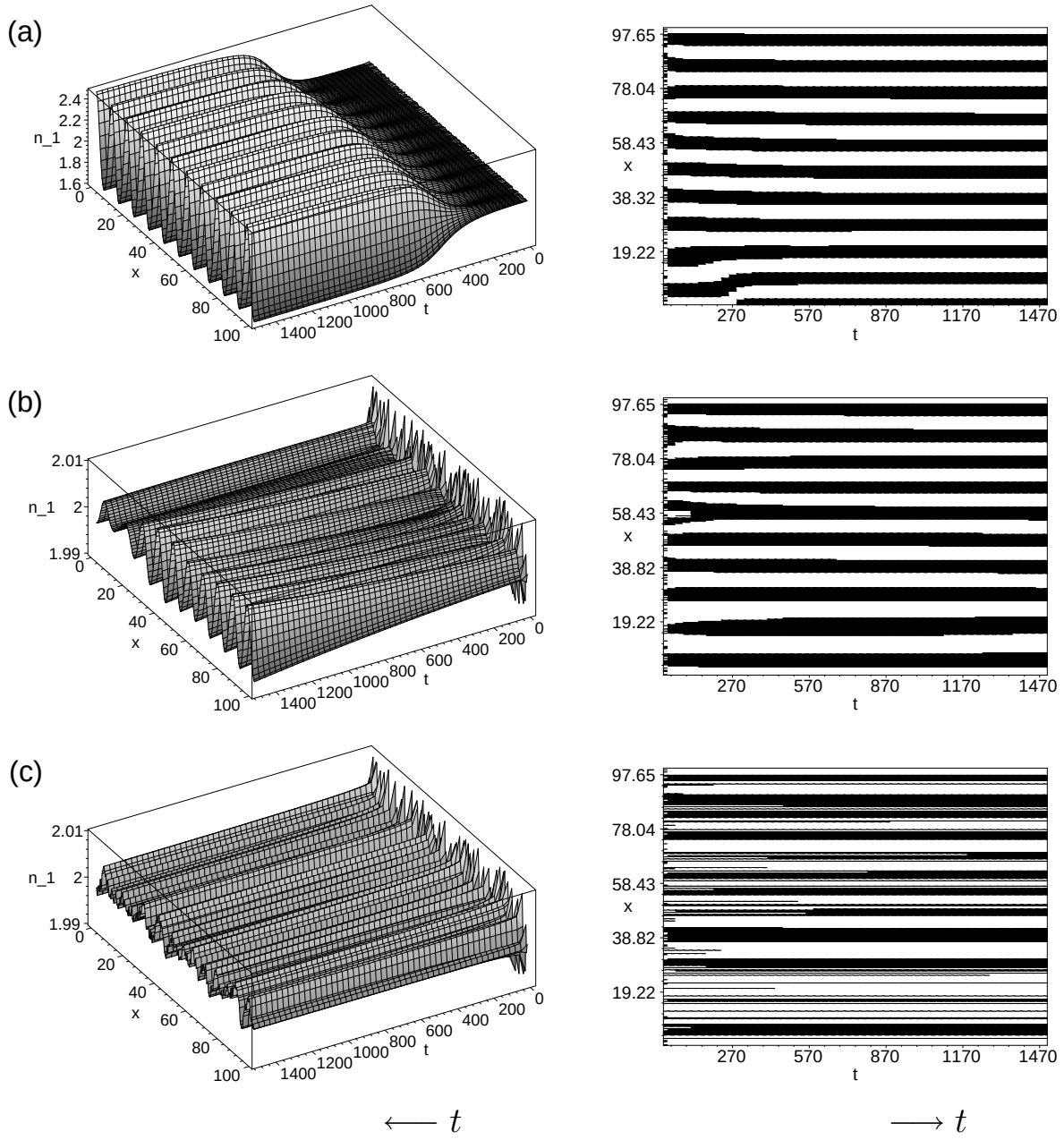

Figure 2. Surface profiles and surface density plots for $n_1(x,t)$ in the fractional Brusselator model with randomly perturbed initial conditions and $d = 25$: (a) $\gamma = 0.8$; (b) $\gamma = 0.5$; (c) $\gamma = 0.2$.

(54) we find $-\ln(u^+(q^\star)) \approx 3.5$ which compares reasonably with the straight line slope of 3.3 in Figure 3.

5. Summary and Conclusions

We revisited the problem of sub-diffusion with reactions within the mesoscopic description of a continuous time random walk with an instantaneous source/sink term.

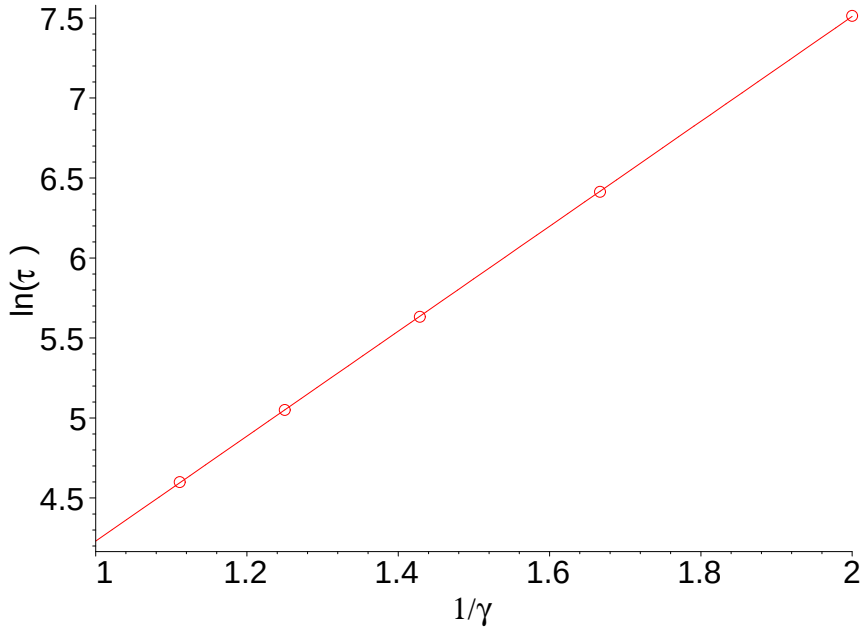

Figure 3. The estimated time for the maximum perturbation to reach 0.01 versus $1/\gamma$ found from the Brusselator model simulations with randomly perturbed initial conditions.

The long time asymptotic limit reduces to a fractional reaction-diffusion equation with fractional order temporal derivatives operating on the diffusion term and an additive source/sink term. We investigated Turing instability induced pattern formation in a two-species variant of this model system with source/sink terms taken to be fractional order temporal derivatives of standard activator-inhibitor kinetics. We also carried out numerical studies of patterning in this system. Our studies showed that the critical diffusivity ratio (activator to inhibitor) for Turing instabilities and the final spatial patterns that emerge are unaffected by the anomalous diffusion in this model. These results are in marked contrast with our earlier studies of Turing pattern formation in fractional activator-inhibitor systems with fractional order temporal derivatives operating on the diffusion term alone [28]. In these earlier studies the anomalous sub-diffusion enables patterning at lower values of the diffusivity ratio (see also the simulations by Weiss [32]) and it yields complex spatio-temporal patterns with arbitrarily small wavelengths excited. In all of our studies of fractional nonlinear reaction-diffusion systems we have found that Turing linear instability analysis is an excellent predictor of both the onset of patterning and the nature of patterning as confirmed in numerical simulations.

The main conclusion of this study should not be that one or other fractional calculus model is the appropriate generic model for anomalously diffusing and reacting species. Different models may be appropriate for different physical situations. Theoretical and numerical studies of the sort undertaken in this paper can help to decide which model is appropriate for a particular physical system. For example if a fractional reaction-diffusion model is sought for the emergence of complex spatio-temporal patterning in

experimental systems with reactions and sub-diffusion then a model with the same fractional order temporal derivative operating on both diffusion terms and reaction terms would not be appropriate.

We are currently developing Monte Carlo simulations for fractional reaction sub-diffusion equations as considered in this paper. Our preliminary Monte Carlo results for sub-diffusion with linear reaction dynamics, which agree with the algebraic results in [30], and extensions for nonlinear reaction dynamics will be the subject of a future publication.

Acknowledgments

This research was supported by the Australian Commonwealth Government ARC Discovery Grants Scheme.

Appendix A. Temporal rescaling of the fractional temporal derivative

In this section we arrive at the expression for the fractional temporal derivative of order $1-\gamma$ of a function of t^γ. Following the approach of Buckwar and Luchko [47] we first write the fractional derivative of a function $y(t) = r(t^\gamma)$ as

$$\frac{\partial^{1-\gamma}}{\partial t^{1-\gamma}} y(t) = \frac{\partial}{\partial t} \frac{1}{\Gamma(\gamma)} \int_0^t \frac{r(\tau^\gamma)}{(t-\tau)^{1-\gamma}} d\tau. \tag{A.1}$$

Now rescaling $\tau = t/\omega$, (A.1) can be written as

$$\frac{\partial^{1-\gamma}}{\partial t^{1-\gamma}} y(t) = \frac{\partial}{\partial t} \frac{t^\gamma}{\Gamma(\gamma)} \int_1^\infty \omega^{-(1+\gamma)} (\omega - 1)^{\gamma-1} r\left(z\omega^{-\gamma}\right) d\omega \tag{A.2}$$

or as

$$\frac{\partial^{1-\gamma}}{\partial t^{1-\gamma}} y(t) = \frac{\partial}{\partial t} t^\gamma \left(K^{1,\gamma}_{-\frac{1}{\gamma}} r\right)(z) \tag{A.3}$$

where the Erdelyi-Kober fractional integral operator is given by

$$\left(K^{\tau,\alpha}_{\beta} r\right)(z) = \begin{cases} \frac{1}{\Gamma(\alpha)} \int_1^\infty \omega^{-(\tau+\alpha)} (\omega-1)^{\alpha-1} r\left(z\omega^{1/\beta}\right) d\omega, & \alpha > 0 \\ r(z), & \alpha = 0 \end{cases}. \tag{A.4}$$

Now applying the product rule to (A.3)

$$\frac{\partial^{1-\gamma}}{\partial t^{1-\gamma}} y(t) = \gamma t^{\gamma-1} \left(K^{1,\gamma}_{-\frac{1}{\gamma}} r\right)(z) + t^\gamma \frac{\partial}{\partial t} \left(K^{1,\gamma}_{-\frac{1}{\gamma}} r\right)(z) \tag{A.5}$$

and using the result in (74) we have

$$\frac{\partial^{1-\gamma}}{\partial t^{1-\gamma}} y(t) = \gamma t^{\gamma-1} \left[1 + z\frac{\partial}{\partial z}\right] \left(K^{1,\gamma}_{-\frac{1}{\gamma}} r\right)(z). \tag{A.6}$$

The fractional derivative can now be written in terms of a Erdelyi-Kober fractional derivative operator

$$\frac{\partial^{1-\gamma}}{\partial t^{1-\gamma}} y(t) = \gamma t^{\gamma-1} \frac{1}{\gamma} \left(P^{\gamma,1-\gamma}_{-\frac{1}{\gamma}} r \right)(z) \tag{A.7}$$

where the Erdelyi-Kober fractional derivative operator is given by

$$\left(P^{\tau,\alpha}_{\beta} r\right)(z) = \prod_{j=0}^{\eta-1} \left(\tau + j - \frac{1}{\beta} z \frac{d}{dz} \right) \left(K^{\tau+\alpha,\eta-\alpha}_{\beta} r \right)(z) \tag{A.8}$$

with $\eta - 1 < \alpha \leq \eta$ and η being a natural number [47].

References

[1] G. Drazer and D.H. Zanette. Experimental evidence of power-law trapping-time distributions in porous media. *Phys. Rev. E*, 60:5858–5864, 1999.

[2] E.R. Weeks and D.A. Weitz. Subdiffusion and the cage effect studied near the colloidal glass transition. *Chem. Phys.*, 284:361–367, 2002.

[3] M. Weiss, H. Hashimoto, and T. Nilsson. Anomalous protein diffusion in living cells as seen by fluorescence correlation spectroscopy. *Biophys. J.*, 84:4043–4052, 2003.

[4] K. Ritchie, X.-Y. Shan, J. Kondo, K. Iwasawa, T. Fujiwara, and A. Kusumi. Detection of non-brownian diffusion in the cell membrane in single molecule tracking. *Biophys. J.*, 88:2266, 2005.

[5] K. Stalinuas. Anticorrelations and subdiffusion in financial systems. *Advances in Complex Systems*, 6:251, 2003.

[6] E. Montroll and G. Weiss. Random walks on lattices ii. *J. Math. Phys.*, 6:167, 1965.

[7] H. Scher and M. Lax. Stochastic transport in a disordered solid. i. theory. *Phys. Rev. B.*, 7:4491–4502, 1973.

[8] R. Metzler and J. Klafter. The random walk's guide to anomalous diffusion: A fractional dynamics approach. *Phys. Rep.*, 339:1–77, 2000.

[9] R. Metzler and J. Klafter. The restaurant at the end of the random walk: Recent developments in the description of anomalous transport by fractional dynamics. *J. Phys. A.*, 37:R161–208, 2004.

[10] I.M. Sokolov and J. Klafter. From diffusion to anomalous diffusion: A century after einstein's brownian motion. *Chaos*, 15:026103, 2005.

[11] D. ben Avraham S. Havlin. *Diffusion and Reactions in Fractals and Disordered Systems.* Cambridge University Press, Cambridge, UK, 2000.

[12] J.D. Murray. *Mathematical Biology. I: An Introduction.* Springer-Verlag, New York, 3rd edition, 2003.

[13] P. Liang. Neurocomputation by reaction-diffusion. *Phys. Rev. Letts.*, 75:1863–1866, 1995.

[14] J.D. Murray. *Mathematical Biology. II: Spatial Models and Biomedical Applications.* Springer-Verlag, New York, 3rd edition, 2003.

[15] J.G. Skellam. Random dispersal in theoretical populations. *Biometrika*, 38(1/2):196–218, 1951.

[16] V. Castets, E. Dulos, J. Boissonade, and P.De Kepper. Experimental evidence of a sustained standing turing-type nonequilibrium chemical pattern. *Phys. Rev. Letts.*, 64:2953–2956, 1990.

[17] B.I. Henry and S.L. Wearne. Fractional reaction-diffusion. *Physica A*, 276:448–455, 2000.

[18] B.I. Henry and S.L. Wearne. Existence of turing instabilities in a two-species fractional reaction-diffusion system. *SIAM Journal of Applied Mathematics*, 62(3):870–887, 2002.

[19] M.O. Vlad and J. Ross. Systematic derivation of reaction-diffusion equations with distributed delays and relations to fractional reaction-diffusion equations and hyperbolic transport equations: application to the theory of neolithic transition. *Physical Review E*, 66:061908, 2002.

[20] S. Fedotov and V. Mendez. Continuous-time random walks and travelling fronts. *Physical Review E*, 66:030102(R), 2002.

[21] J. Sung, E. Barkai, R.J. Silbey, and S. Lee. Fractional dynamics approach to diffusion-assisted reactions. *J. Chem. Phys.*, 116:2338–2341, 2002.

[22] K. Seki, M. Wojcik, and M. Tachiya. Fractional reaction-diffusion equation. *Journal of Chemical Physics*, 119(4):2165–2170, 2003.

[23] K. Seki, M. Wojcik, and M. Tachiya. Recombination kinetics in subdiffusive media. *Journal of Chemical Physics*, 119(14):7525–7533, 2003.

[24] M. Fukunaga. Numerical solutions of fractional diffusion equation with source term. *Int. J. Appl. Math*, 14:269–295, 2003.

[25] S.B. Yuste, L. Acedo, and K. Lindenberg. Reaction front in an $A + B \to C$ reaction-subdiffusion process. *Phys. Rev. E*, 69:036126, 2004.

[26] V. Mendez, D. Campos, and S. Fedotov. Front propagation in reaction-dispersal models with finite jump speed. *Phys. Rev. E.*, 70:036121, 2004.

[27] V. Mendez and V. Ortega-Cejas. Front propagation in hyperbolic fractional reaction-diffusion equations. *Phys. Rev. E*, 71:057105, 2005.

[28] B.I. Henry, T.A.M. Langlands, and S.L. Wearne. Turing pattern formation in fractional activator-inhibitor systems. *Phys. Rev. E*, 72:026101, 2005.

[29] V.V. Gafiychuk and B.Yo. Datsko. Pattern formation in a fractional reaction-diffusion system. *Physica A*, 365:300–306, 2006.

[30] B.I. Henry, T.A.M. Langlands, and S.L. Wearne. Anomalous diffusion with linear reaction dynamics: From continuous time random walks to fractional reaction-diffusion equations. *Physical Review E*, 2006, in press.

[31] I.M. Sokolov, M.G.W. Schmidt, and F. Sagues. Reaction sub-diffusion equations. *Phys. Rev. E*, 73:031102, 2006.

[32] M. Weiss. Stabilizing turing patterns with subdiffusion in systems with low particle numbers. *Phys. Rev. E*, 68:036213, 2003.

[33] C. Varea and R.A. Barrio. Travelling turing patterns with anomalous diffusion. *J. Phys. C: Condens. Matter*, 16:S5081–S5090, 2004.

[34] D. del-Castillo-Negrete, B.A. Carreras, and V.E. Lynch. Front dynamics in reaction-diffusion systems with levy flights: A fractional diffusion approach. *Phys. Rev. Lett.*, 91:018302, 2003.

[35] K. Pearson. The problem of the random walk. *Nature*, 72:294, 1905.

[36] J. Klafter, A. Blumen, and M.F. Shlesinger. Stochastic pathway to anomalous diffusion. *Phys. Rev. A*, 35:3081, 1987.

[37] G. Hornung, B. Berkowitz, and N. Barkai. Morphogen gradient formation in a complex environment: An anomalous diffusion model. *Phys. Rev. E*, 72:041916, 2005.

[38] W. Feller. *An Introduction to Probability Theory and its Applications. Vol II.* Wiley, New York, 2nd edition, 1966.

[39] G. Margolin and B. Berkowitz. Continuous time random walks revisited: first passage time and spatial distributions. *Physica A.*, 334:46–66, 2004.

[40] E. Scalas, R. Gorenflo, F. Mainardi, and M. Raberto. Revisiting the derivation of the fractional diffusion equation. *Fractals*, 11:281, 2003.

[41] I. Prigogine and R. Lefever. Symmetry breaking instabilities in dissipative systems ii. *J. Chem. Phys*, 48:1695–1700, 1968.

[42] A. Gierer and H. Meinhardt. A theory of biological pattern formation. *Kybernetika*, 12:30–39, 1972.

[43] I. Podlubny. *Fractional Differential Equations*, volume 198 of *Mathematics in Science and Engineering*. Academic Press, New York and London, 1999.

[44] A. Erdélyi, editor. *Higher Transcendental Functions*, volume 3. McGraw-Hill, New York, 1955.

[45] R.B. Paris. Exponential asymptotics of the Mittag-Leffler function. *Proc. R. Soc. Lond. A*, 458(2028):3041–3052, 2002.

[46] R. Wong and Y.-Q. Zhao. Exponential Asymptotics of the Mittag-Leffler function. *Constr. Approx.*, 18:355–385, 2002.

[47] E. Buckwar and Y. Luchko. Invariance of a partial differential equation of fractional order under the lie group of scaling transformations. *J. Math Anal Appl.*, 227:81–97, 1998.

[48] K.B. Oldham and J. Spanier. *The Fractional Calculus: Theory and Applications of Differentiation and Integration to Arbitrary Order*, volume 111 of *Mathematics in Science and Engineering*. Academic Press, New York and London, 1974.

[49] T.A.M. Langlands and B.I. Henry. The accuracy and stability of an implicit solution method for the fractional diffusion equation. *J. Comput. Phys.*, 205:719, 2005.